

[Osada, K., Y. Shido, H. Iida and M. Kido, Deposition processes of ionic constituents to snow cover, Atmospheric Environment, 44, 347-353, January 2010.](#)

## Deposition processes of ionic constituents to snow cover

K. Osada<sup>#1</sup>, Y. Shido<sup>\*1</sup>, H. Iida<sup>2</sup>, and M. Kido<sup>3</sup>

1: Graduate School of Environmental Studies, Nagoya University,  
Nagoya, 464-8601, Japan

2: Tateyama Caldera SABO Museum,  
Tateyama, 930-1405, Japan

3: Toyama Prefectural Environmental Science Research Center,  
Imizu, 939-0363, Japan

# corresponding author: kosada@nagoya-u.jp

Phone: +81-52-788-6049, FAX: +81-52-789-4306

\* Now at: Toyota Tsusho Corporation, Tokyo, Japan

Keywords: Acid deposition, Scavenging process, Eastern Asia, Mountain slope, Mount Tateyama.

## Abstract

Atmospheric deposition is an important removal process of aerosol particles and gases from the atmosphere. To elucidate the relative contributions of wet and dry processes and in-cloud and below-cloud scavenging based on deposition amounts in winter at Mt. Tateyama, central Japan, we obtained daily samples (December, 2006 – March, 2007) of size-segregated aerosol particles and precipitation at Senjyugahara (SJ; 475 m a.s.l.) and vertical samples of spring snow cover at Murododaira (MR, 2450 m a.s.l., 13 km distance from SJ) on the western flank of Mt. Tateyama. The  $\text{NH}_4^+$  and  $\text{nssSO}_4^{2-}$  in aerosols were mostly found in the fine fraction ( $< 2 \mu\text{m}$ ), although  $\text{Na}^+$ ,  $\text{NO}_3^-$ , and  $\text{nssCa}^{2+}$  were mainly detected in the coarse fraction ( $> 2 \mu\text{m}$ ). Average ionic concentrations ( $\mu\text{g}\cdot\text{g}^{-1}$ ) in precipitation at SJ were higher about 3.8 for  $\text{Na}^+$  and  $\text{nssCa}^{2+}$ , 3.4 for  $\text{NO}_3^-$ , 3.7 for  $\text{NH}_4^+$ , 2.5 for  $\text{nssSO}_4^{2-}$  than those at MR, whereas cumulative precipitation amounts at SJ and MR were, respectively, 84 and 175 cm of water equivalent. Wet and dry deposition amounts during the study period were estimated for sites using size-segregated aerosol data, winter averages of  $\text{HNO}_3$ ,  $\text{NH}_3$ , and  $\text{SO}_2$  concentrations, and dry deposition velocities. Particle dry deposition comprised about 3% ( $\text{Na}^+$ ) to 11% ( $\text{NH}_4^+$ ) of the total deposition at MR. The maximum amounts of gas dry deposition were estimated, respectively, as 4, 13, and 3% of the total deposition at MR for  $\text{NH}_4^+$ ,  $\text{NO}_3^-$ , and  $\text{nssSO}_4^{2-}$ . The relative contributions of below-cloud scavenging (BCS) between MR and SJ were estimated as considering the wet only deposition amount at MR. Higher contributions of BCS were obtained for  $\text{Na}^+$  (56%) and  $\text{nssCa}^{2+}$  (45%), whereas BCSs for  $\text{NH}_4^+$ ,  $\text{NO}_3^-$ , and  $\text{nssSO}_4^{2-}$  were lower than 28%. Ionic constituents existing predominantly in the coarse fraction showed a large contribution of BCS.

## 1 Introduction

Snow is a major type of precipitation that commonly occurs over wide regions of middle and high latitudes during winter. At subzero temperatures, fallen snow accumulates on the ground, forming snow cover. Such snow cover often contains a record of the chemistry in the atmosphere during snow formation and subsequent accumulation (Junge, 1977). Incorporation of atmospheric aerosol particles and water-soluble gases into snow cover is a complex process that is generally classified into wet and dry processes (Davidson et al., 1996). The wet process is related to formation and deposition with hydrometeors. It consists of in-cloud and below-cloud scavenging processes according to the location of inclusion. In-cloud scavenging includes nucleation, uptake during subsequent growth, and impaction processes for particles and dissolution of water-soluble gases within clouds. Below-cloud scavenging is the capture of aerosol particles and gases by hydrometeors after leaving the cloud base. Through a process known as dry deposition, aerosol particles and gases are also incorporated into snow cover without precipitation. Although wet deposition occurs only during discrete time intervals of precipitation, dry deposition occurs continuously. To date, these scavenging processes have been studied through field observations, laboratory experiments, and theoretical considerations (Pruppacher and Klett, 1997; Zufall and Davidson, 1998; Jennings, 1998; Seinfeld and Pandis, 2006, references are therein). However, the relative contributions of the processes to deposition are difficult to infer from field measurements because of their complexity.

Several field experiments have been undertaken to separate in-cloud and below-cloud contributions in wet scavenging processes (Murakami et al., 1983; Zinder et al., 1988; Oberholzer et al., 1993; Katsuno et al., 1996). Such studies use the altitude difference between mountaintops and lowlands to separate in-cloud and below-cloud scavenging. The

spatial distribution of precipitation amounts around a mountain varies with orographical and meteorological conditions (Charlson et al., 1988; Barry and Chorly, 2003). Precipitation shows wide variation of concentrations in individual samples. Therefore, caution is necessary in interpreting such an estimation based on individual precipitation events (Baltensperger et al., 1993).

The northwest side of Honshu Island's Japanese Alps, which faces the Sea of Japan, has heavy snowfall during winter because of strong northwesterly winds (Arakawa and Taga, 1969). Mount Tateyama (3015 m a.s.l.) is located in the Hida range of the northern Japanese Alps (Fig. 1). Snow cover at Mt. Tateyama in spring is about 6–10 m; it remains during November–July. The air temperature is rarely above freezing during November–April (Nakagawa et al., 1976). Snow cover prevents the windblown redistribution of local soil materials on the ground and anthropogenic pollution sources are absent near the mountain. Therefore, the snow cover at Mt. Tateyama provides useful information related to total deposition of atmospheric aerosol particles (aeolian dusts and ammonium sulfate etc.) and water-soluble gases ( $\text{SO}_2$ ,  $\text{HNO}_3$ ,  $\text{NH}_3$ , etc.) transported far from the Asian continent with less influence from local emission sources (Osada et al., 2004).

On the other hand, emissions of anthropogenic pollutants such as  $\text{NO}_x$ ,  $\text{SO}_2$ ,  $\text{NH}_3$ , and other related aerosol species are increasing because of economic growth, especially in Asia (Streets et al., 2003; Akimoto, 2003; Ohara et al., 2007). Increased anthropogenic emissions might engender increased wet and dry deposition flux at leeward areas such as the Japanese archipelago (Uno et al., 2007). Although wet and dry deposition monitoring (Acid Deposition Monitoring Network in East Asia – EANET <http://www.eanet.cc/index.html>) has been performed at several sites in eastern Asia including Japan, deposition processes of atmospheric chemicals to snow cover in the receptor area are not well understood (Okita et al., 1996; Fujita et al., 2003; Seto et al., 2007). Understanding deposition processes is particularly important for modeling and predicting the long-range transport of pollutants and other atmospheric aerosols and for evaluating environmental effects of acidic deposition (Textor et al., 2006; Wang et al., 2008).

To elucidate the relative contributions of wet and dry processes at a high elevation site, and to investigate in-cloud and below-cloud scavenging processes at the windward side of Mt. Tateyama, we obtained daily samples of size-segregated aerosol particles and precipitation at Senjugahara ( $36^\circ 35' \text{N}$ ,  $137^\circ 27' \text{E}$ , 475 m a.s.l.) and spring snow samples accumulated at Murododaira ( $36^\circ 35' \text{N}$ ,  $137^\circ 36' \text{E}$ , 2450 m a.s.l.), on the western flank of Mt. Tateyama. We estimated the deposition flux of  $\text{Na}^+$ ,  $\text{nssCa}^{2+}$ ,  $\text{NO}_3^-$ ,  $\text{NH}_4^+$ , and  $\text{nssSO}_4^{2-}$  at sites including the dry deposition amount for aerosol particles based on aerosol data. Dry deposition amounts for gaseous species ( $\text{HNO}_3$ ,  $\text{NH}_3$ , and  $\text{SO}_2$ ) were also calculated and combined with particle-dry deposition to subtract from the total deposition at MR. Finally, we discuss the relative contribution of below-cloud scavenging to the deposition amount at SJ.

## 2 Samples and laboratory analysis

Figure 1

Figure 1 portrays a location map of Mt. Tateyama (3015 m), Japan with two sampling sites, Senjugahara (475 m, abbreviated to SJ hereinafter), and Murododaira (2450 m, MR). The SJ site is about 20 km southeast from the city of Toyama and from the Toyama Bay area, and 13 km west of MR. The difference of altitude between the two sites is 1975 m. No large urban or industrial area exists near the mountain. Because of its proximity, a similar precipitation condition would be expected for the sites.

Aerosol particles were collected daily at SJ from 22 December 2006 to 17 April 2007. Daily aerosol samples were changed every 9 AM. Aerosol particles were segregated into two size ranges using a two-stage stacked filter pack (47 mm diameter, NILU). The filter pack consisted of a Nuclepore polycarbonate filter of 8.0  $\mu\text{m}$  pore size (Corning Coster Corp.) and a Teflon membrane filter of 1.0  $\mu\text{m}$  nominal pore size (Advantec Toyo Kaisha Ltd.) at a flow rate of ca. 15 L  $\text{min}^{-1}$ . The equivalent aerodynamic diameter for 50% collection efficiency of the Nuclepore filter was estimated as approximately 2  $\mu\text{m}$  (John et al., 1983). The equivalent aerodynamic diameter is expected to vary with the particle type. Stacked filter packs similar to those used in this study were widely used for separating coarse ( $> 2 \mu\text{m}$ ) and fine ( $< 2 \mu\text{m}$ ) aerosols (e.g., Andreae et al., 1988; Kim et al., 1988). The efficiency of the particle size separation by the stacked filter is evident in the fact that most of the sea-salt component is found on the first stage (see Section 3.1 below). The sample air flow rate was measured using a mass flow meter (SEF-51; STEC Inc. now Horiba Stec Co. Ltd.) that was calibrated for 25°C and 1013 hPa.

At SJ, daily precipitation (mostly snowfall) was also collected by manually changing precipitation collectors at 9 AM each day. A fallen snow collector and/or a bucket with a polyethylene bag inside for rain were used to collect precipitation samples depending on the precipitation type. We used a movable snow stake with a flat board as a new snow collector. We collected daily increments of new snow falling on the board above an old snow surface. Consulting with weather forecasts, appropriate collector, sometimes both collectors, were set to sample precipitation at SJ. Precipitation samples at SJ were stored in a freezer.

At MR, vertical snow samples were obtained from hand-dug pits on November 29, 2006 and March 15, 2007. A flat tableland of about 200  $\times$  200 m and an open view lie to the west side toward the Sea of Japan. Therefore, the snow deposition environment at MR is suitable for continuous snow accumulation (Osada et al., 2004). In general, the air temperature at MR remains at less than 0°C from late November to late March. We worked on the snow pits before the snow melted because chemical constituents can be redistributed by water percolation. Details of snow sampling at MR are available elsewhere (Osada et al., 2004). We collected a series of vertically continuous snow samples, typically about 100 g, in 10-cm increments using a precleaned stainless steel shovel (cylindrical body with a skew cut edge, 7 cm in diameter and 10 cm long with a handle of 10 cm long) and polyethylene gloves. The samples were stored in Whirl-Pak bags (NASCO) and kept frozen until further analysis. Snow density was measured using a constant volume (100  $\text{cm}^3$ ) snow sampler for the same horizontal layers to estimate the water equivalent height of snow cover. Triplicate snow samples (300  $\text{cm}^3$ ) were combined and weighed for density calculations. Reproducibility of multiple snow density measurements of the same horizontal snow layer is better than 5%.

In the laboratory at Nagoya University, melt water samples were filtered using a membrane filter (0.45  $\mu\text{m}$  pore size, 13AI; GL Science Inc.) before ionic chemical analysis using ion chromatography (DX-300; Dionex Corp. and LC-10A; Shimadzu Corp.). Procedural blank samples for the Whirl-Pak bags and aerosols were treated identically to actual snow and aerosol samples. Concentrations of these procedural blanks were mostly negligible but, when present, they were subtracted from the values in the actual sample. Analytical errors determined from replicate measurements of chemical standards are within 10% of the average concentration levels of samples used for this study. Details of laboratory analyses were reported by Kido et al. (2001) and Osada et al. (2007). Non-sea-salt (nss) concentrations of  $\text{SO}_4^{2-}$  and  $\text{Ca}^{2+}$  were estimated from  $\text{Na}^+$  contents in the sample according to their respective ratios in seawater (Wilson, 1975).

We measured the number concentrations of atmospheric aerosol particles using laser particle counters (KC-01C; Rion Co. Ltd.) at MR and SJ. The laser particle counter continuously measures the number of aerosol particles for five diameter ranges: larger than 0.3, 0.5, 1.0, 2.0, and 5.0  $\mu\text{m}$ . For aerosol at MR, we installed a snow clogging preventer at the tip of the inlet utilizing wind vibration to make a clearance of air flow channel. Details of the continuous aerosol measurements are found elsewhere (Osada et al., 2003).

### 3 Results and discussion

Figure 2

#### 3.1 Ionic constituents in aerosol particles at SJ and their size distributions

Figure 2 depicts temporal variations of ionic constituents ( $\text{nmol}\cdot\text{m}^{-3}$ ) in aerosol particles at SJ from December 22, 2006 to March 15, 2007. High  $\text{Na}^+$  concentrations were often observed with strong winds over the Sea of Japan, as reported previously (Suzuki and Tsunogai, 1988; Satake and Yamane, 1992). The  $\text{nssCa}^{2+}$  concentration was high on February 6–8, 2007. Although no KOSA (advection of Asian dust) phenomenon was reported by a nearby meteorological observatory for these days, the higher  $\text{nssCa}^{2+}$  suggests the influence of Asian dust (Ichikuni, 1978; Osada et al., 2007). Concentrations of  $\text{NO}_3^-$ ,  $\text{NH}_4^+$ , and  $\text{nssSO}_4^{2-}$  also showed a high peak during this period. Results show that  $\text{NH}_4^+$  and  $\text{nssSO}_4^{2-}$  were mostly found in the fine fraction ( $< 2 \mu\text{m}$ ), whereas  $\text{Na}^+$ ,  $\text{NO}_3^-$ , and  $\text{nssCa}^{2+}$  were detected mainly in the coarse fraction ( $> 2 \mu\text{m}$ ).

Figure 3 presents a scatter plot of  $\text{Cl}^-$ ,  $\text{Mg}^{2+}$ , and  $\text{Cl}^-$  plus  $\text{NO}_3^-$  versus the  $\text{Na}^+$  concentration of the coarse ( $> 2 \mu\text{m}$ ) size fraction at SJ. Coefficients of correlation for  $\text{Cl}^-$  and  $\text{Mg}^{2+}$  versus  $\text{Na}^+$  concentration were very good ( $r^2$ : 0.94 and 0.92, respectively), suggesting that these three ions have a common source such as sea salts. The slope of  $\text{Mg}^{2+}$  versus  $\text{Na}^+$  (0.12) was close to the seawater ratio (blue line, 0.11) but that of  $\text{Cl}^-$  versus  $\text{Na}^+$  (0.91) was slightly lower than the seawater ratio (red line, 1.16). Adding  $\text{NO}_3^-$  to  $\text{Cl}^-$  concentration increased the slope to 1.19, which is very close to the seawater ratio. This fact suggests that  $\text{NO}_3^-$  in the coarse fraction might be formed by the reaction of coarse sea-salt particles with  $\text{HNO}_3$  gas in the atmosphere (e.g., Mamane and Gottlieb, 1992; Roth and Oelert, 1999) and/or on the filter during sampling (e.g., Kitto and Colbeck, 1999).

Figure 3

#### 3.2 Ionic constituents in precipitation at SJ

Figure 4

Figure 4 presents temporal variations of ionic constituents ( $\mu\text{g}\cdot\text{g}^{-1}$ ) in precipitation at SJ from December 3, 2006 to March 15, 2007. Because of the manual setting of the snow and rain collectors, some precipitation events were not obtained for this study but the acquisition rate of daily samples compared to continuous meteorological data was 92%. As indicated by light blue lines in Fig. 4, lower ionic concentrations existed in samples of large daily precipitation amounts similar to dilution effects (Junge, 1977). However, some samples (such as those of January 7 and February 4 as indicated by green lines) showed higher  $\text{Na}^+$  concentrations as opposed to large daily precipitation. On these days, strong winds were reported in this region, suggesting active production of sea-salt aerosols to the atmosphere. Although sea salt ( $\text{Na}^+$ ) concentrations in aerosols for these days were not so high at SJ, a large amount of sea salt aerosols might be scavenged through precipitation and deposited to this area.

### 3.3 Vertical profiles of ionic constituents in snow at MR

Figure 5

Figure 5 presents vertical profiles of ionic concentrations ( $\mu\text{g}\cdot\text{g}^{-1}$ ) in snow cover at MR as a function of the water equivalent height (WEH). According to depth-density data of the earlier snow pit on November 29, 2006, lower 50 cm of WEH in March corresponds to snow deposited before the end of November. This is shown as a horizontal dotted line in Fig. 5. A large peak of  $\text{Na}^+$  concentration was observed at 80–90 cm of WEH. Concentration of  $\text{nssCa}^{2+}$  showed peaks at 70–80, 185, and 195 cm. Concentrations of  $\text{NO}_3^-$ ,  $\text{NH}_4^+$ , and  $\text{nssSO}_4^{2-}$  showed some mutual similarities in vertical profiles: low at about 55 and 200 cm, and high at 70, 110, 135, 160, and 185 cm etc. The comparison of profiles between MR and SJ is not straightforward because of the irregularity of the event frequency and the amount of precipitation but some correlation is apparent; combination peaks for  $\text{nssCa}^{2+}$  and  $\text{Na}^+$  at 70–90 in MR might correspond to peaks in late December to early January at SJ, and the broad increase of  $\text{NO}_3^-$ ,  $\text{NH}_4^+$ , and  $\text{nssSO}_4^{2-}$  concentrations at MR might match with frequently high periods in late January to mid-February at SJ.

On the other hand, compared with average concentrations ( $\mu\text{g}\cdot\text{g}^{-1}$ ) at SJ in Fig. 4, values at SJ were higher about 3.8 for  $\text{Na}^+$  and  $\text{nssCa}^{2+}$ , 3.4 for  $\text{NO}_3^-$ , 3.7 for  $\text{NH}_4^+$ , 2.5 for  $\text{nssSO}_4^{2-}$  than those of MR. The total precipitation amount from December 1, 2006 to March 15, 2007 at SJ was 84 cm of water, whereas WEH above the December horizon (50 cm) at MR was 175 cm, namely, precipitation that had fallen onto the ground was 2.1 times higher at MR than SJ. Orographic precipitation effects might engender this increase of precipitation amount at high elevation sites because of nearly continuous westerly winds forcing for orographic lift of humid winter monsoon air from the Sea of Japan.

### 3.4 Deposition amount during the study period

Table 1

Table 1 presents the amount of deposition during December 1 – March 15 at SJ and MR. The amount of deposition for the period was calculated as the sum of products between concentration and precipitation amount of individual event at SJ and the sum of products between concentration and WEH of snow samples at MR. Values at MR were limited for samples from the upper 175 cm of WEH. The SJ/MR ratios of deposition amount ( $\text{g}\cdot\text{m}^{-2}$ ) were 2.2 for  $\text{Na}^+$ , 1.7 for  $\text{nssCa}^{2+}$ , 1.1 for  $\text{NO}_3^-$ , and 1.2 for  $\text{NH}_4^+$ , but the deposition of  $\text{nssSO}_4^{2-}$  at MR was slightly higher than at SJ (SJ/MR=0.82). Compared with the results of aerosol measurements presented in Fig. 2, ions of higher SJ/MR ratios were found mostly in coarse mode particles, although ratios close to unity were obtained for ions detected in fine mode. Larger particles might have a greater contribution to dry deposition and below-cloud scavenging (Jennings, 1998). Precipitation samples at SJ can be considered mostly as wet deposition with less influence of dry deposition. Therefore, the observed SJ/MR relation with particle size implies that the deposition amount at SJ might be influenced by below-cloud scavenging of aerosols. On the other hand, the deposition amount at MR includes dry deposition during the non-precipitation period. Consequently, this study examines relative contributions of (1) dry deposition to snow at MR and (2) below-cloud scavenging between MR and SJ.

### 3.4.1 Particle and gas dry deposition

Dry deposition flux ( $F_{dpi}$ ) of  $i$  species of ion in aerosol particles was estimated as

$$F_{dpi} = v_{dpf} \cdot C_{ipf} + v_{dpc} \cdot C_{ipc}, \quad (1)$$

where  $v_{dpf}$  and  $v_{dpc}$  are deposition velocities for fine ( $< 2 \mu\text{m}$ ) and coarse ( $> 2 \mu\text{m}$ ) particles, and where  $C_{ipf}$  and  $C_{ipc}$  respectively represent average ionic concentrations of  $i$  species for fine and coarse fractions of aerosols. Although the deposition velocity might vary with various meteorological and surface conditions, we simply applied 0.2 and 1.0 cm/s, respectively, for  $v_{dpf}$  and  $v_{dpc}$  (Duce et al., 1991).

To estimate amounts of particle dry deposition at MR from aerosols data at SJ, we assume a uniform vertical distribution of aerosols between SJ and MR. Figure 6 presents an example of time variations in February 2007 at the sites for fine ( $> 0.3 \mu\text{m}$ ) and coarse ( $> 2 \mu\text{m}$ ) aerosol concentrations and amounts of hourly precipitation at SJ. Although some discrepancies during precipitation were apparent, such as during 7–10, 14–16, and 23 February, aerosol concentrations of fine and coarse particles were nearly uniform between the sites; their temporal variations showed synchronicity. Aerosol concentrations at SJ were occasionally higher than those at MR, probably because of the influence of sea salts and other aerosols emitted from earth's surface, which are generally rich at lower altitudes. Consequently, our estimate of aerosol dry deposition for MR using aerosol data at SJ should be considered as the maximum contribution.

Finally, we obtained the deposition amount through particle dry deposition for the period of 105 days (December 1 – March 15). As presented in Table 1, the amount of dry deposition by aerosols comprises about 3% ( $\text{Na}^+$ ) to 11% ( $\text{NH}_4^+$ ) of total deposition at MR.

Dry deposition flux of gaseous species was estimated similarly using the deposition velocity and average concentration of gaseous species during winter. Various  $v_d$  for gases have been reported for many kinds of surfaces (e.g., Dewalle, 1987; Cadle, 1991; Warneck, 1999). Values of  $v_d$  for gases on cold snow surface depend also on meteorological (such as temperature) parameters (Wesely, 1989) and might be much lower than  $0.1 \text{ cm}\cdot\text{s}^{-1}$  at cold temperatures. On the other hand, higher  $v_d$  for  $\text{HNO}_3$  on snow surface was reported in the literature (Cadle et al., 1985). Therefore, we estimate the range (zero to maximum) of gaseous dry deposition amount at MR using fastest values of  $v_d$  on snow as  $1.4 \text{ cm}\cdot\text{s}^{-1}$  for  $\text{HNO}_3$  and  $0.15 \text{ cm}\cdot\text{s}^{-1}$  for  $\text{SO}_2$  (Cadle et al., 1985). For  $\text{NH}_3$ , report of  $v_d$  on snow surface was very limited. Therefore, we use  $0.7 \text{ cm}\cdot\text{s}^{-1}$  as the maximum value on turf grassland (Hayashi et al., 2006).

Average concentrations of gases at MR were assumed as averages between December 2006 and March 2007 at Happo Station, a remote mountain site under EANET (ca. 27 km north–northeast of Mt. Tateyama,  $36^\circ 42' \text{N}$ ,  $137^\circ 48' \text{E}$ , 1850 m a.s.l.). Average concentrations were  $0.2 \pm 0.0$  ppbv for  $\text{NH}_3$ ,  $0.3 \pm 0.1$  ppbv for  $\text{HNO}_3$ , and  $1.1 \pm 0.2$  ppbv for  $\text{SO}_2$ . Gas concentrations at Happo Station were not so different from those ( $0.1 \pm 0.1$  ppbv for  $\text{NH}_3$ ,  $0.1 \pm 0.1$  ppbv for  $\text{HNO}_3$ , and  $0.9 \pm 0.2$  ppbv for  $\text{SO}_2$ ) for the same period at Sado-seki (ca. 180 km north–northeast of Happo Station,  $38^\circ 15' \text{N}$ ,  $138^\circ 24' \text{E}$ , 136 m a.s.l.), another EANET station on a solitary island, Sado Island, in the Sea of Japan. This similarity enables us to assume uniform distribution of these gases over this area. Details of site descriptions and data reports of EANET stations are available at the web site (<http://www.eanet.cc/product.html>).

Estimated maximum gas dry deposition amounts for 105 days are presented in Table 1. Amounts of gas dry deposition respectively comprise, at most, 4, 13, and 3% of total deposition at MR for  $\text{NH}_4^+$ ,  $\text{NO}_3^-$ , and  $\text{nssSO}_4^{2-}$ . The sum of dry position amounts for

particles and gases comprises 3% for  $\text{Na}^+$ , 8% for  $\text{nssCa}^{2+}$ , 11–14% for  $\text{NH}_4^+$ , 5–18% for  $\text{NO}_3^-$ , and 5–9% for  $\text{nssSO}_4^{2-}$  of total deposition amount at MR, depending on magnitudes (zero to maximum assumed) of  $v_d$  for gases.

### 3.4.2 Below-cloud scavenging

During precipitation, although the site MR is mostly located within cloud cover, the cloud base is always higher than the site SJ. Although the exact height of the cloud base might vary according to meteorological conditions, precipitation received at SJ might include below-cloud scavenging from altitudes at MR to SJ. To evaluate the contribution of below-cloud scavenging, the wet only amount of deposition at MR ( $\text{MR}_{\text{wet}}$ ) was made by subtracting dry deposition from total deposition at MR (Table 1). Then, the contribution of below-cloud scavenging (BCS) in percentage terms for deposition at SJ is estimated as

$$\text{BCS} = 100 \times \frac{(\text{SJ} - \text{MR}_{\text{wet}})}{\text{SJ}}. \quad (2)$$

As presented in Table 1, higher BCSs were obtained for  $\text{Na}^+$  (56%) and  $\text{nssCa}^{2+}$  (45%), which were predominantly found in the coarse fraction. The BCSs for  $\text{NH}_4^+$ ,  $\text{NO}_3^-$ , and  $\text{nssSO}_4^{2-}$  were, respectively, 22–25, 18–28, and -15 – -11 in percentage terms. The observed tendency of higher BCSs for coarser particles agrees well with results of previous studies (Murakami et al., 1983; Zinder et al., 1988). Although the relative contributions of BCS reported in Murakami et al. (1983) at Mt. Teine are similar, the altitude difference between the sites is almost double for this study: BCSs per unit distance (BCS/km) are all less than 30% in this study. The values of BCS/km in this study agree with the results for non-fog conditions described by Zinder et al. (1988).

Although most  $\text{NO}_3^-$  in aerosols were found in the coarse fraction (Fig. 2), much lower BCS comparing with those of  $\text{Na}^+$  and  $\text{nssCa}^{2+}$  was obtained. This might result from sampling artifact as influenced by the reaction between gaseous  $\text{HNO}_3$  and  $\text{NaCl}$  to form  $\text{NaNO}_3$  on Nuclepore filters during aerosol sampling. The collection efficiency of aerosols by raindrops or snowflakes is low in fine mode particles (Jennings, 1998). Lower BCS for  $\text{NO}_3^-$  might be explained if the dominant size fraction of  $\text{NO}_3^-$  at SJ were in fine mode. On the other hand, BCSs for  $\text{nssSO}_4^{2-}$  were negative values (-15 – -11%), implying greater than assumed additional deposition of  $\text{nssSO}_4^{2-}$ . Fumarolic gases ( $\text{H}_2\text{S}$  etc.) in Jigoku-dani (Mizutani et al., 2000) near MR might engender additional  $\text{SO}_4^{2-}$  deposition onto snow at MR, but very low  $v_d$  for gaseous deposition is expected for low temperatures.

### 3.5 Implications for modeling studies

Recently, chemical transport models (CTMs) have become important tools to explore air pollution transport pathways and to assess the impact of long-range transport. However, additional studies including better treatments of scavenging processes have been suggested for improving the model performance of CTMs on deposition amount (Textor et al., 2006; Wang et al., 2008). Although numerical models for simulating below-cloud scavenging have been reported (Feng, 2009; Henzing et al., 2006), the degrees of scavenging and concentration are expected to vary among individual precipitation cases (Baltensperger et al., 1993). Consequently, instead of individual approaches, we have specifically examined average conditions of deposition during winter. The estimated contribution rate in this study

will be useful to evaluate the CTM performance, especially for long-term assessment of various deposition species.

#### 4 Summary and Conclusions

Daily samples of size-segregated aerosol particles and snowfall—at Senjyugahara (SJ, 475 m a.s.l.) from December 2006 through March 2007 and spring snow samples at Murododaira (MR, 2450 m a.s.l.) on the western flank of Mt. Tateyama, Japan—were collected to assess the relative contributions of various deposition processes of major ionic constituents in snow cover. For aerosol samples,  $\text{NH}_4^+$  and  $\text{nssSO}_4^{2-}$  were mostly found in the fine fraction ( $< 2 \mu\text{m}$ ), whereas  $\text{Na}^+$ ,  $\text{NO}_3^-$ , and  $\text{nssCa}^{2+}$  were detected mainly in the coarse fraction ( $> 2 \mu\text{m}$ ). Assuming the deposition velocity, the particle dry deposition amount during the study period was estimated from size-segregated aerosol data. Particle dry deposition comprised about 3 ( $\text{Na}^+$ ) to 11% ( $\text{NH}_4^+$ ) of total deposition at MR. Similarly, maximum amounts of gas dry deposition for  $\text{HNO}_3$ ,  $\text{NH}_3$ , and  $\text{SO}_2$  were estimated using maximum deposition velocities on snow and average gas concentrations at Happo Station near the site for the same period. The amounts of gas dry deposition respectively comprised 4, 13, and 3%, at maximum, of total deposition at MR for  $\text{NH}_4^+$ ,  $\text{NO}_3^-$ , and  $\text{nssSO}_4^{2-}$ .

The relative contributions of below-cloud scavenging (BCS) between MR and SJ were estimated by comparing the deposition amount at SJ with wet only deposition at MR ( $\text{MR}_{\text{wet}}$ ) subtracting dry depositions from the total at MR. Higher contributions of BCS per kilometer were obtained for  $\text{Na}^+$  (28%) and  $\text{nssCa}^{2+}$  (23%), whereas lower BCSs (11–13%, 9–14% and -8 – -5%) were obtained, respectively, for  $\text{NH}_4^+$ ,  $\text{NO}_3^-$ , and  $\text{nssSO}_4^{2-}$ . Ionic constituents existing predominantly in the coarse fraction showed a large contribution of BCS. Results related to the relative contributions of BCSs in this study will be useful for evaluating the performance of chemical transport models.

#### Acknowledgements

We are grateful to Messrs. E. Saeki, O. Tagaya, and T. Kitamura, who assisted with snow observations in severe weather conditions. We are indebted to the staff of Tateyama Kurobe Kanko (TKK) and the Tateyama Caldera SABO Museum for assisting our work at Mt. Tateyama. This work was performed with the support of a Grant-in-Aid for Scientific Research in Priority Areas, Grant No. 18067005 (W-PASS), provided by the Ministry of Education, Culture, Sports, Science and Technology, Japan, and by Grants-in-Aid for Scientific Research (B) 20310009 and (A) 20244078 from the Ministry of Education, Culture, Sports, Science and Technology. This research is a contribution of IGBP/SOLAS activity.

#### References

- Akimoto, H., 2003. Global air quality and pollution. *Science* 302, 1716–1719.
- Andreae, M.O., Berresheim, H., Andreae, T.W., Kritz, M.A., Bates, T.S., Merrill, J.T., 1988. Vertical distribution of dimethylsulfide, sulfur dioxide, aerosol ions, and radon over the northeast Pacific Ocean. *Journal of Atmospheric Chemistry* 6, 149–173.
- Arakawa, H., Taga, H., 1969. Climate of Japan, in: Arakawa, H. (Ed.), *Climates of Northern and Eastern Asia*. World Survey of Climatology, vol. 8, Elsevier, Amsterdam, 119–131.

- Baltensperger, U., Schwikowski, M., Gäggeler, H.W., Jost, D.T., Beer, J., Siegenthaler, U., Wagenbach, D., Hofmann, H.J., Synal, H.A., 1993. Transfer of atmospheric constituents into an alpine snow field. *Atmospheric Environment* 27A, 1881–1890.
- Barry, R.G., Chorley, R.J., 2003. *Atmosphere, Weather and Climate*, 8th edition, Routledge, London, pp. 80–84.
- Cadle, S.H., Dasch, J.M., Mulawa, P., 1985. Atmospheric concentrations and the deposition velocity to snow of nitric acid, sulphur dioxide and various particulate species. *Atmospheric Environment* 19, 1819–1827.
- Cadle, S.H., 1991. Dry deposition to snowpacks, in: Davies, T. D. et al. (Eds.), *Seasonal snowpacks*, NATO ASI Series, G 28, Springer-Verlag, Berlin, pp. 21–66.
- Charlson, R.J., Twohy, C.H., Quinn, P.K., 1988. Physical influence of altitude on the chemical properties of cloud and of water deposited from the troposphere, in: Unsworth, M. H. and Fowler, D. (Eds.), *Acid Deposition at High Elevation Sites*, NATO ASI Series C 252, Kluwer Academic, Dordrecht, pp. 109–124.
- Davidson, C.I., Bergin, M.H., Kuhn, H.D., 1996. The deposition of particles and gases to ice sheets, in: Wolff, E.R. and Bales, R.C. (Eds.), *Chemical Exchange between the Atmosphere and Polar Snow*, NATO ASI Series, Vol. I 43, Springer, Berlin, pp. 275–306.
- Dewalle, D.R., 1987. Review of snowpack chemistry, in: Jones, H. G. and Orville-Thomas, W. J. (Eds.), *Seasonal snowcovers: Physics, Chemistry, Hydrology*, NATO ASI Series, C 211, Reidel, Dordrecht, pp. 255–268.
- Duce, R.A., Liss, P.S., Merrill, J.T., Atlas, E.L., Buat-Menard, P., Hicks, B.B., Miller, J.M., Prospero, J.M., Ariomoto, R., Church, T.M., Ellis, W., Galloway, J.N., Hansen, L., Jickells, T.D., Knap, A.H., Reinhardt, K.H., Schneider, B., Soudine, A., Tokos, J.J., Tsunogai, S., Wollet, R., Zhou, M., 1991. The atmospheric input of trace species to the world ocean. *Global Biogeochemical Cycles* 5, 193–259.
- Feng, J., 2009. A size-resolved model for below-cloud scavenging of aerosols by snowfall. *Journal of Geophysical Research* 114, doi:10.1029/2008JD011012.
- Fujita, S., Takahashi, A., Sakurai, T., 2003. The wet deposition of acid and some major ions over the Japanese Archipelago. *Tellus* 55B, 23–34.
- Hayashi, K., Komada, M., Miyata, A., 2006. Estimation of dry deposition of ammoniacal nitrogen using an inferential method – effects of ammonia volatilization through plant stomata and surface wetness on dry deposition velocity. *Journal of Japanese Society of Atmospheric Environment* 41, 78–90. (in Japanese)
- Henzing, J.S., Olivie, D.J.L., van Velthoven, P.F.J., 2006. A parameterization of size resolved below cloud scavenging of aerosols by rain. *Atmospheric Chemistry and Physics* 6, 3363–3375.
- Ichikuni, M., 1978. Calcite as a source of excess calcium in rainwater. *Journal of Geophysical Research* 83, 6249–6252.
- Jennings, S.G., 1998. Wet processes affecting atmospheric aerosols. in: Harrison, R., M. Van Grieken, R. (Eds.), *Atmospheric Particles*, John Wiley & Sons, Chichester, pp. 475–507.
- John, W., Hering, S., Reischl, G., Sasaki, G., Goren, S., 1983. Characteristics of Nuclepore filters with large pore size—II. Filtration properties. *Atmospheric Environment* 17, 373–382.

- Junge, C.E., 1977. Processes responsible for the trace content in precipitation. in: *Isotopes and impurities in snow and ice*, IAHS Publ., 118, pp. 63–77, 1977.
- Katsuno, T., Satsumabayashi, H., Sasaki, K., Shikano, M., Ohta, M., Hatakeyama, S., Murano, K., 1996. Chemical components of airborne particulate matter and acid deposition in Happono and Nagano City. *Journal of Japanese Society of Atmospheric Environment* 31, 282–291 (in Japanese).
- Kido M., Osada, K., Matsunaga, K., Iwasaka, Y., 2001. Diurnal variation of ionic aerosol species and water-soluble gas concentrations at a high-elevation site in the Japanese Alps. *Journal of Geophysical Research* 106, 17335–17345.
- Kim, Y.J., Sievering H., Boatman, J.F., 1988. Airborne measurement of atmospheric aerosol particles in the lower troposphere over the central United States. *Journal of Geophysical Research* 93, 12631–12644.
- Kitto, A-M.N., Colbeck, I., 1999. Filtration and denuder sampling techniques. In: Spurny, K. R. (Ed.), *Analytical chemistry of aerosols*, Lewis Publications, Boca Raton, pp. 103–132.
- Mamane, Y., Gottlieb, J., 1992. Nitrate formation on sea-salt and mineral particles – a single particle approach. *Atmospheric Environment* 26A, 1763–1769.
- Mizutani, Y., Sasaki, Y., Hori, M., Koyama, M., 2000. Chemical compositions and isotopic ratios of fumarolic gases and hot spring waters from Tateyama-jigokudani, Toyama, Japan. *Chikyukagaku (Geochemistry)* 34, 77–89 (in Japanese).
- Murakami, M., Kimura, T., Magono, C., Kikuchi, K., 1983. Observations of precipitation scavenging for water-soluble particles. *Journal of Meteorological Society of Japan* 61, 346–358.
- Nakagawa, M., Kawada, K., Okabe, T., Shimizu, H., Akitaya, E. 1976. Physical properties of the snow cover on Mt. Tateyama in central Honshu, Japan. *Seppyo* 38, 1–8. (in Japanese with English summary)
- Oberholzer, B., Volken, M., Collet, J.L.Jr., Staehelin, J., Waldvogel, A., 1993. Pollutant concentrations and below-cloud scavenging of selected N (-III) species along a mountain slope, *Water, Air, and Soil Pollution* 68, 59–73.
- Ohara, T., Akimoto, H., Kurokawa, J., Horii, N., Yamaji, K., Hayasaka, T., 2007. An Asian emission inventory of anthropogenic emission sources for the period 1980–2020. *Atmospheric Chemistry and Physics* 7, 4419–4444.
- Okita, T., Hara, H., Fukuzaki, N., 1996. Measurements of atmospheric SO<sub>2</sub> and SO<sub>4</sub><sup>2-</sup>, and determination of the wet scavenging coefficient of sulfate aerosols for the winter monsoon season over the sea of Japan, *Atmospheric Environment* 30, 3733–3739.
- Osada, K., Kido, M., Iida, H., Matsunaga, K., Iwasaka, Y., Nagatani, M., Nakada, H., 2003. Seasonal variation of free tropospheric aerosol particles at Mt. Tateyama, central Japan. *Journal of Geophysical Research* 108, doi:10.1029/2003JD003544.
- Osada, K., Iida, H., Kido, M., Matsunaga, K., Iwasaka, Y., 2004. Mineral dust layers in snow at Mount Tateyama, Central Japan: formation processes and characteristics. *Tellus* 56B, 382–392.

- Osada, K., Kido, M., Nishita, C., Matsunaga, K., Iwasaka, Y., Nagatani, M., Nakada, H., 2007. Temporal variation of water-soluble ions of free tropospheric aerosol particles over central Japan. *Tellus* 59B, 742–754.
- Pruppacher, H.R., Klett, J.D., 1997. *Cloud Chemistry*, in: *Microphysics of Clouds and Precipitation*, 2nd edition, Kluwer Academic, Dordrecht, pp. 700–791.
- Roth, B., Okada, K., 1998. On the modification of sea-salt particles in the coastal atmosphere. *Atmospheric Environment* 32, 1555–1569.
- Satake, H., Yamane, T., 1992. Deposition of non-sea-salt sulphate observed at Toyama facing the Sea of Japan for the period of 1981–1991. *Geochemical Journal* 26, 299–305.
- Seinfeld, J.H., Pandis, S.N., 2006. *Dry Deposition and Wet Deposition*, in: *Atmospheric Chemistry and Physics*, 2nd edition, John Wiley & Sons, Hoboken, pp. 900–979.
- Seto, S., Sato, M., Tatano, T., Kusakari, T., Hara, H., 2007. Spatical distribution and source identification of wet deposition at remote EANET sites in Japan. *Atmospheric Environment* 41, 9386–9396.
- Streets, D.G., Bond, T.C., Carmichael, G.R., Fernandes, S.D., Fu, Q., He, D., Klimont, Z., Nelson, S.M., Tsai, N.Y., Wang, M.Q., Woo, J.-H., Yarber, K.F., 2003. An inventory of gaseous and primary aerosol emissions in Asia in 2000. *Journal of Geophysical Research* 108, doi: 10.1029/2002JD003093.
- Suzuki, T., Tsunogai, S., 1998. Daily variation of aerosols of marine and continental origin in the surface air over a small island, Okushiri, in the Japan Sea. *Tellus* 40B, 42–49.
- Textor, C. and 40 others, Analysis and quantification of the diversities of aerosol life cycles within AeroCom. *Atmospheric Chemistry and Physics* 6, 1777–1813.
- Uno, I., Uematsu, M., Hara, Y., He, Y. J., Ohara, T., Mori, A., Kamaya, T., Murano, K., Sadanaga, Y., Bandow, H., 2007. Numerical study of the atmospheric input of anthropogenic total nitrate to the marginal seas in the western North Pacific region. *Geophysical Research Letters* 34, L17817, doi:10.1029/2007GL030338.
- Wang, Z., Xie, F., Sakurai, T., Ueda, H., Han, Z., Carmichael, G. R., Streets, D., Engardt, M., Holloway, T., Hayami, H., Kajino, M., Thongboonchoo, N., Bennet, C., Park, S. U., Fung, C., Chang, A., Sartelet, K., Amann, M., 2008. MICS-Asia II: Model inter-comparison and evaluation of acid deposition. *Atmospheric Environment* 42, 3528–3542.
- Warneck, P., 1999. *Fundamentals*, in: Zeller, R. et al. (Eds.), *Global aspects of atmospheric chemistry*, Springer, New York, pp. 1–20.
- Wesely, M.L., 1989. Parameterization of surface resistances to gaseous dry deposition in regional-scale numerical models. *Atmospheric Environment* 23, 1293–1304.
- Wilson, T.R.S., 1975. Salinity and the major elements of seawater. in: Riley, J. P., Skirrow, G., (Eds.), *Chemical Oceanography*, vol. 1, Academic Press, San Diego, pp. 365–413.
- Zinder, B., Schumann, T., Waldvogel, A., 1988. Aerosol and hydrometeor concentrations and their chemical composition during winter precipitation along a mountain slope – II. Enhancement of below-cloud scavenging in stably stratified atmosphere. *Atmospheric Environment* 22, 2741–2750.
- Zufall, M.J., Davidson, C.I., 1998. *Dry Deposition of Particles*. in: Harrison, R.M., Van Grieken, R. E., (Eds.), *Atmospheric Particles*. John Wiley & Sons, Chichester, pp. 425–473.

Table 1 Observed deposition amount, estimated dry deposition, and contribution of below cloud scavenging (%): Dec. 1, 2006 – Mar. 15, 2007.

site	Na <sup>+</sup> g m <sup>-2</sup>	nssCa <sup>2+</sup> g m <sup>-2</sup>	NH <sub>4</sub> <sup>+</sup> g m <sup>-2</sup>	NO <sub>3</sub> <sup>-</sup> g m <sup>-2</sup>	nssSO <sub>4</sub> <sup>2-</sup> g m <sup>-2</sup>
SJ	2.49±0.14	0.20±0.01	0.32±0.01	0.97±0.03	1.53±0.05
MR	1.12±0.04	0.12±0.01	0.28±0.01	0.84±0.02	1.86±0.04
Dry, Particle	0.03±0.03	0.01±0.01	0.03±0.02	0.04±0.05	0.10±0.05
Dry, Gas ( $v_{dg}$ max)	–	–	0.01±0.00	0.11±0.05	0.06±0.01
Sum of Dry Deposition	0.03	0.01	0.03 <sup>#</sup> –0.04	0.04 <sup>#</sup> –0.15	0.10 <sup>#</sup> –0.16
MR <sub>wet</sub>	1.09	0.11	0.24–0.25	0.69–0.80	1.70–1.76
SJ/MR <sub>wet</sub>	2.26	1.82	1.28–1.33	1.21–1.40	0.87–0.90
BCS* (%)	56	45	22–25	18–28	-15– -11
BCS/km (%)	28	23	11–13	9–14	-8 – -5

# values for  $v_{dg}=0$  and  $v_{dg}$  max

\* BSC: below-cloud scavenging

## Figure Captions

Figure 1(a) Map of Mount Tateyama in Japan. (b) Schematic diagram of Senjyugahara and Murododaira observation sites on the mountain slope.

Figure 2 Temporal variations of size-segregated ionic concentrations ( $\mu\text{g}\cdot\text{m}^{-3}$ ) at Senjyugahara during December 2006 – March 2007. Green and red colors denote size ranges of  $> 2 \mu\text{m}$  and  $< 2 \mu\text{m}$ , respectively. Major ticks in the horizontal axis are shown from 31 day intervals from December 1, 2006.

Figure 3 Scatter plot of  $\text{Cl}^-$ ,  $\text{Mg}^{2+}$ , and  $\text{Cl}^-$  plus  $\text{NO}_3^-$  versus  $\text{Na}^+$  concentration of coarse ( $> 2 \mu\text{m}$ ) size fraction at SJ. Red and blue lines represent molar ratios in seawater (1.16 for  $\text{Cl}^-/\text{Na}^+$  and 0.11 for  $\text{Mg}^{2+}/\text{Na}^+$ , respectively).

Figure 4 Temporal variations of daily precipitation amount ( $\text{mm}\cdot\text{day}^{-1}$ ) and ionic concentrations ( $\mu\text{g}\cdot\text{g}^{-1}$ ) in precipitation samples at SJ. See text for blue and green lines.

Figure 5 Vertical profiles of ionic concentrations ( $\mu\text{g}\cdot\text{g}^{-1}$ ) of snow cover at MR obtained on March 15, 2007 as a function of the water equivalent height from the ground. The horizontal dotted line represents the horizon as of the end of November 2006 (see the text).

Figure 6 Comparison of aerosol number concentrations ( $> 0.3$  and  $> 1.0 \mu\text{m}$ ) at SJ (solid lines) and MR (cross), and hourly precipitation (vertical bar) at SJ.

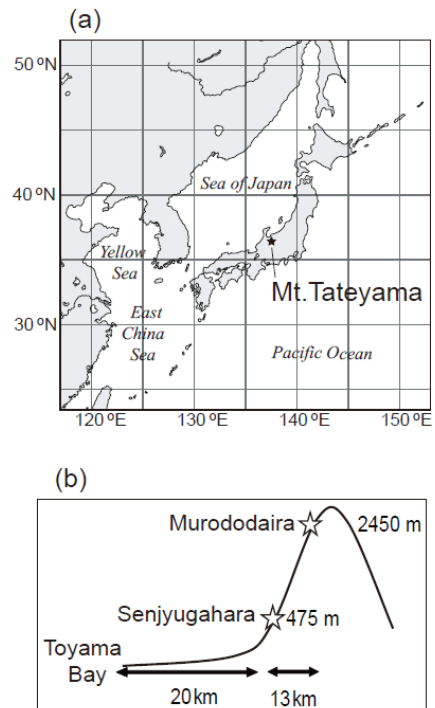


Figure 1(a) Map of Mount Tateyama in Japan. (b) Schematic diagram of Senjyugahara and Murododaira observation sites on the mountain slope.

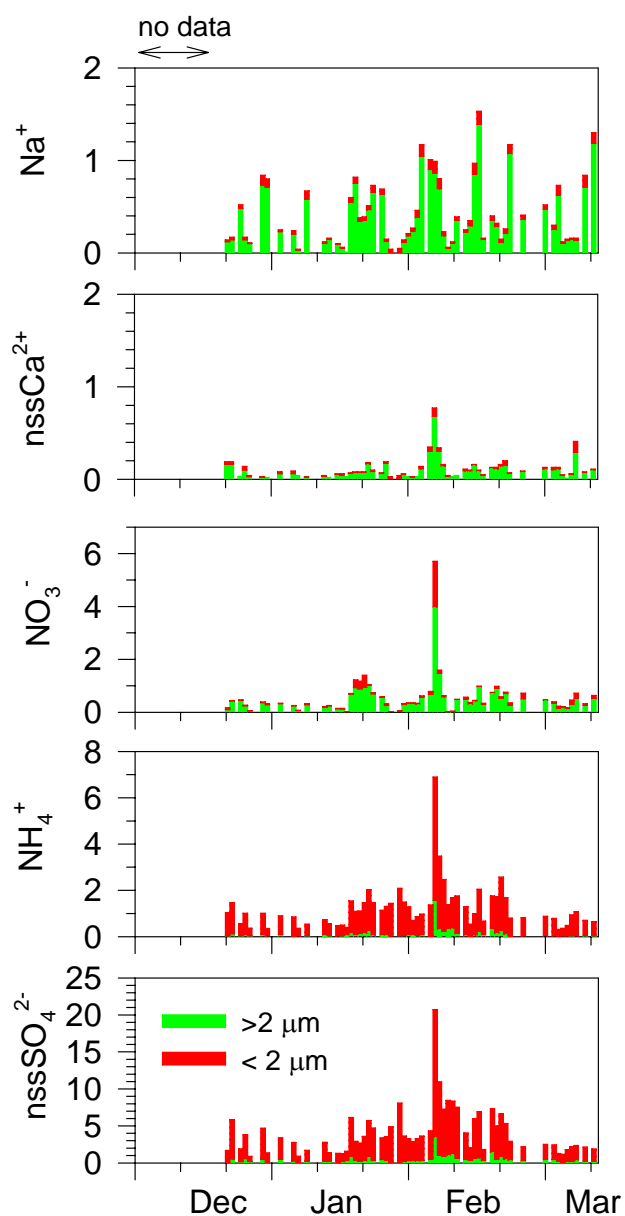


Figure 2 Temporal variations of size-segregated ionic concentrations ( $\mu\text{g}/\text{m}^3$ ) at Senjugahara during December 2006 – March 2007. Green and red colors denote size ranges of  $> 2 \mu\text{m}$  and  $< 2 \mu\text{m}$ , respectively. Major ticks in the horizontal axis are shown from 31 day intervals from December 1, 2006.

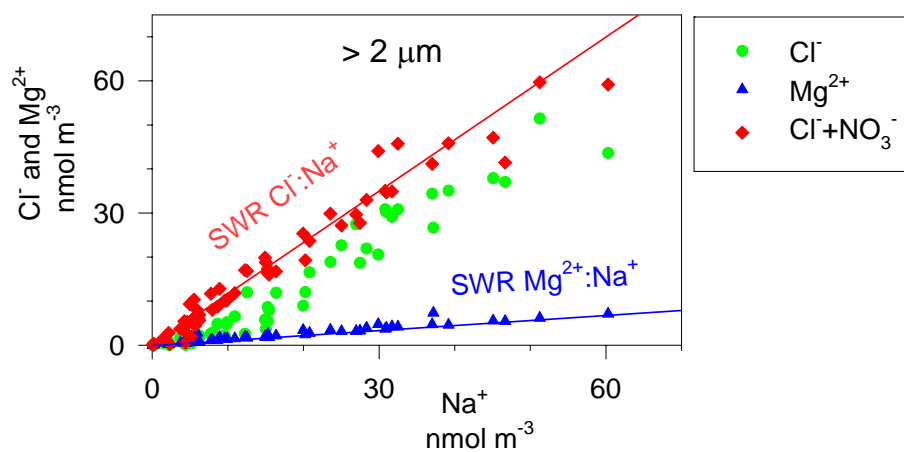


Figure 3 Scatter plot of Cl<sup>-</sup>, Mg<sup>2+</sup>, and Cl<sup>-</sup> plus NO<sub>3</sub><sup>-</sup> versus Na<sup>+</sup> concentration of coarse (> 2 μm) size fraction at SJ. Red and blue lines represent molar ratios in seawater (1.16 for Cl<sup>-</sup>/Na<sup>+</sup> and 0.11 for Mg<sup>2+</sup>/Na<sup>+</sup>, respectively).

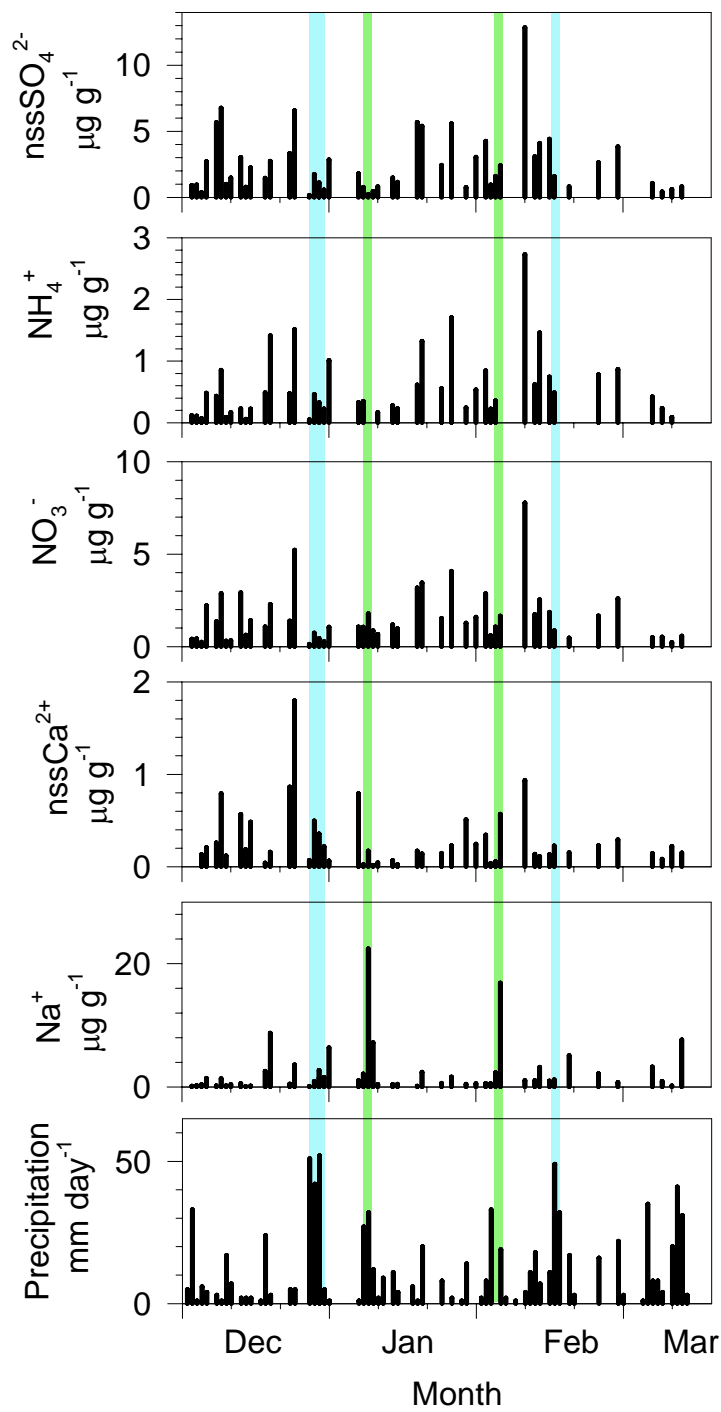


Figure 4 Temporal variations of daily precipitation amount ( $\text{mm day}^{-1}$ ) and ionic concentrations ( $\mu\text{g}\cdot\text{g}^{-1}$ ) in precipitation samples at SJ. See text for blue and green lines.

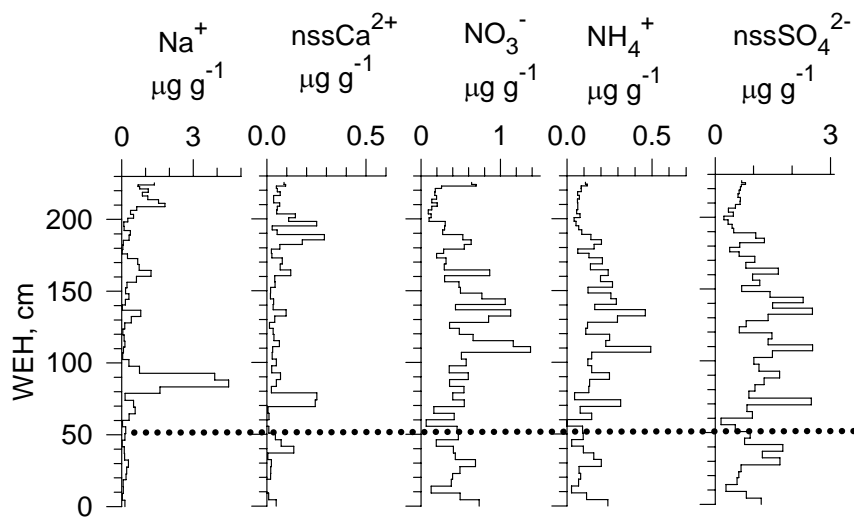


Figure 5 Vertical profiles of ionic concentrations ( $\mu\text{g}\cdot\text{g}^{-1}$ ) of snow cover at MR obtained on March 15, 2007 as a function of the water equivalent height from the ground. The horizontal dotted line represents the horizon as of the end of November 2006 (see the text).

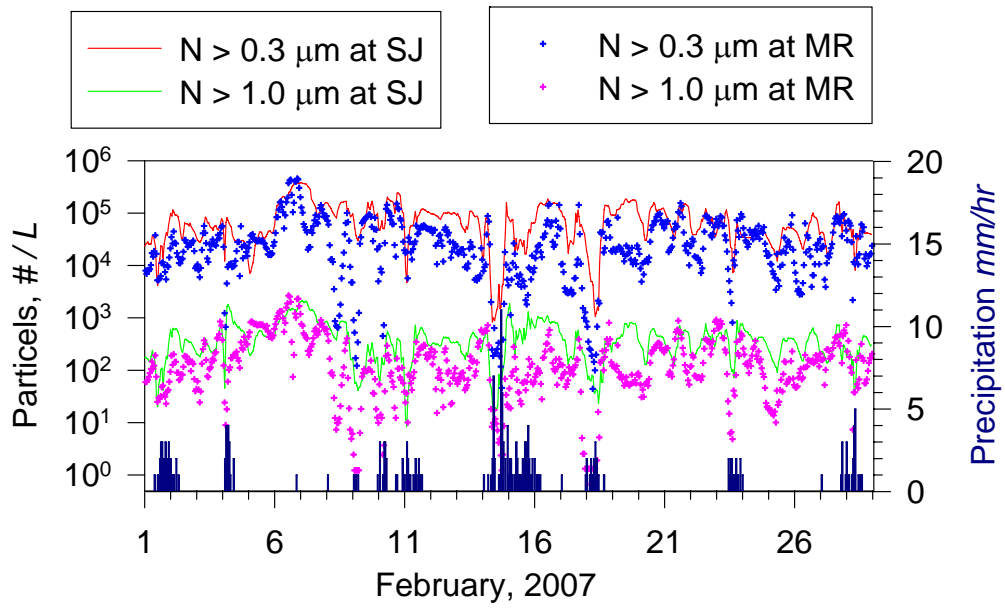


Figure 6 Comparison of aerosol number concentrations ( $> 0.3$  and  $> 1.0$   $\mu\text{m}$ ) at SJ (solid lines) and MR (cross), and hourly precipitation (vertical bar) at SJ.